Biosensors and Bioelectronics 128 (2019) 83–90

Contents lists available at ScienceDirect

Biosensors and Bioelectronics

journal homepage: www.elsevier.com/locate/bios

Focusing aptamer selection on the glycan structure of prostate-specific antigen: Toward more specific detection of prostate cancer☆

Ana Díaz-Fernández[a,b], Rebeca Miranda-Castro[a,b], Noemí de-los-Santos-Álvarez[a,b], Eloy Fernández Rodríguez[c], María Jesús Lobo-Castañón[a,b,*]

[a] Dpto. Química Física y Analítica, Universidad de Oviedo, Av. Julián Clavería 8, 33006 Oviedo, Spain
[b] Instituto de Investigación Sanitaria del Principado de Asturias, Avenida de Roma, 33011 Oviedo, Spain
[c] Hospital Universitario de Cabueñes, C/ Los Prados, 395, 33394 Gijón, Asturias, Spain

ARTICLE INFO

Keywords:
Aptamer
Cancer detection
Electrochemical biosensor
Glycosylation
Prostate-specific antigen
SELEX

ABSTRACT

The development of chemical sensors capable of detecting the specific glycosylation patterns of proteins offers a powerful mean for the early detection of cancer. Unfortunately, this strategy is scarcely explored because receptors recognizing the glycans linked to proteins are challenging to discover. In this work, we describe a simple method for directing the selection of aptamers toward the glycan structure of the glycoproteins, with prostate-specific antigen (PSA) as a model target. Using this strategy, we identified one aptamer (PSA-1) that binds the glycan moiety of PSA with reasonable affinity (a dissociation constant of 177 ± 65 nM). Interestingly, an electrochemical sensor with a sandwich format employing the identified aptamer as a signaling receptor, provides a tool of discriminating human PSA from the unglycosylated protein, with a limit of detection of 0.66 ng/mL. The sensor responds to different levels of PSA in serum, correlating well with chemiluminescence ELISA used in hospitals even with higher potential to discriminate clinically meaningful prostate cancer. Although validation on a larger cohort is needed, this is the first demonstration of an aptamer-based sensor to detect PSA by focusing in its glycan moiety

1. Introduction

Changes in the glycosylation pattern of cell surface and secreted glycoproteins are common in malignant transformations and cancer progression (Munkley and Elliot, 2016), and there is growing evidence that these alterations are associated with the acquisition of all the cancer hallmarks presently accepted (Hanahan and Weinberg, 2011). In fact, the majority of tumor markers currently used in clinic are glycoproteins. This is the case of prostate-specific antigen (PSA), the gold standard option for diagnosing and predicting progression of prostate cancer, which is the most prevalent cancer in men in Europe and USA (Siegel et al., 2018). Since the adoption of PSA test for prostate cancer screening in the early 1990s, the number of patients diagnosed at an early stage has dramatically increased. However, the reduced specificity of the total PSA test leads to overdetection of indolent cancers, resulting in a large number of unnecessary biopsies and overtreatment (Hayes and Barry, 2014).

A major goal of research in prostate cancer detection has been the development of screening methodologies with improved specificity, which enables to distinguish between clinically significant and insignificant prostatic adenocarcinoma. Toward this goal, total PSA test is complemented with other parameters such as free PSA, PSA isoform specific detection and PSA kinetics (Lilja et al., 2008), but the search continues for more accurate prostate cancer biomarkers.

A promising approach for improving the specificity of PSA for cancer detection is to analyze the aberrant PSA glycosylation pattern (Gilgunn et al., 2013). Recent advances in the field of glycobiology have demonstrated that during tumorigenesis subtle changes in the glycan structure of PSA occur (Saldova et al., 2011; Tabarés et al., 2006), which may allow to distinguish PSA from normal and tumor cells. The detection of these specific glycosylation changes may confer a new perspective for clinical applications, although the lack of glyco-specific antibodies constitutes a major obstacle. Nature offers a group of glycan-binding proteins i.e. lectins, which have been used in enzyme-linked lectin assays and microarrays for detecting the glycan moiety of PSA (Jolly et al., 2016; Li et al., 2011; Meany et al., 2009; Pihíková et al., 2016). However, these receptors capable of recognizing a specific glycan structure, are not directed against the glycosylation site (the

☆ Dedicated in memory of Prof. Emil Palecek.

* Corresponding author.
E-mail address: mjlc@uniovi.es (M.J. Lobo-Castañón).

https://doi.org/10.1016/j.bios.2018.12.040
Received 6 November 2018; Received in revised form 10 December 2018; Accepted 21 December 2018
Available online 26 December 2018
0956-5663/

glycan and its surrounding in the protein), with the subsequent low level of discrimination among different glycoproteins with similar glycan structures. In addition, the usefulness of lectins is limited by their low affinity, usually in the μM range. Therefore, there is an urgent need for the development of new receptors with high affinity and selectivity for the glycosylation site of glycoprotein biomarkers such as PSA. The synthetic receptors termed aptamers (also referred to as chemical antibodies) have surfaced as a promising alternative to natural ones. There are different strategies and techniques to adapt the selection of aptamers to the requirements of the target, with the possibility of directing the recognition toward the domain or region of interest in a much simpler and efficient way than in the case of antibodies production. The rational tailoring of aptamers for the glycosylation site of the glycoprotein may provide new diagnostic tools for early detection of cancer (Díaz-Fernández et al., 2018).

There are different aptamers developed against PSA, both DNA (Hsieh et al., 2017; Li et al., 2018; Park et al., 2016; Savory et al., 2010) and RNA oligonucleotides (Jeong et al., 2010; Svobodova et al., 2013), but the approaches used for their selection do not have the ability to direct them toward the recognition of the carbohydrate structure of PSA. Consequently, aptamer-based sensors described so far provide information on total PSA, but are insensitive to changes in the glycosylation pattern (Cha et al., 2014; Heydari-Brafrooei and Shamszadeh, 2017; Souada et al., 2015; Tamboli et al., 2016; Tzouvadaki et al., 2016; Yang et al., 2017; Zhao and Ma, 2018).

To focus the aptamer selection to the carbohydrate substructure of glycoproteins, only one approach has been described, which was applied to fibrinogen (Li et al., 2008). It relies on the ability of boronic acids to interact with diols and requires the incorporation of boronic acid-modified nucleotides during the selection. However, boronic acid-glycan interactions play a key role in the recognition of the glycoprotein by the resulting aptamers, rendering them less selective for discriminating subtle changes in the glycan structure.

Motivated by the above arguments, we describe here the first aptamer selection directed toward a native glycan structure of proteins, without the need for modified nucleotides. Our approach relies on the use of rationally designed counter-selections targeting the non-glycosylated protein, thus removing from the selection pool the oligonucleotides that recognize the protein by positions different from the glycosylation site. Counter-SELEX is an approach used to evolve aptamers with exquisite selectivity against the desired target. This procedure involves challenging the DNA library against a structurally related compound, for example a protein isoform, using the unbound sequences for the posterior round of selection (Miranda-Castro et al., 2016). Rose et al. (2010) synthesized a short peptide surrounding the VEGF glycosite and attached a single sugar (N-acetylglucosamine) as a target for SELEX, using the unglycosylated peptide to direct the selection. Though this work demonstrated the feasibility of this approach with 50-fold discrimination power, the aptamer was not challenged to the native protein containing a vast more complex sugar chain (polysaccharide). Similarly, aptamers against glucose-bound hemoglobin have been identified very recently (Eissa and Zourob, 2017).

The new aptamers we identify are employed as signaling receptors in a sandwich electrochemical aptasensor for the detection of PSA. The evaluation of the clinical performance of the aptasensor in serum at different PSA levels suggests it may be a promising approach to improve the cancer specificity of PSA analysis.

2. Materials and methods

2.1. Immobilization of proteins for SELEX

Proteins were immobilized on the surface of Dynabeads M-280 tosylactivated magnetic particles (Invitrogen). 165 μL (5 mg) of the beads were washed with 1 mL of BM (19 mM NaH_2PO_4, 81 mM Na_2HPO_4 pH 7.4), and incubated with 100 μg of the protein in 100 μL of BM2 (3 M $(NH_4)_2SO_4$ pH 7.4) in a Thermomixer for 12–18 h at 37 °C at 1300 rpm. After magnetic separation, the particles were conditioned in 1 mL of BLmod (PBS 1 × + 0.5% BSA) for 1 h at 37 °C at 1300 rpm. Finally, the particles were washed twice with 1 mL of BLmod2 (PBS 1 × + 0.1% BSA) and resuspended in 250 μL of BLmod2 for long-term storing at 4 °C. To estimate the amount of immobilized protein the unbound protein was quantified by Bradford assay (Supporting information). Using this protocol, the magnetic particles were modified with BSA, human PSA (hPSA) and recombinant PSA (rPSA) for negative (no target, BSA-MPs), positive (with target, hPSA-MPs) and counter-selection steps (non-glycosylated target, rPSA-MPs), respectively.

2.2. SELEX procedure

The ssDNA library consisted of a 40 nucleotides randomized central region flanked at both ends by two constant sequences of 20 nucleotides each, for hybridization with PCR primers during amplification (Table S1). 1 nmol of the starting DNA library in 1 mL of the selection buffer (BS: PBS 1 × pH 7.4) was heated at 95 °C for 4 min and then quickly cooled in ice for 4 min. BSA-MPs were added to this solution, maintaining the amount of immobilized protein 10-fold lower than the amount of DNA. A concentration of 1.23 μg/mL of BSA and 1.23 μg/mL of tRNA was also added to minimize unspecific binding and as a competitor, respectively. The [tRNA]/[DNA] ratio was kept at 0.1. After interaction and magnetic separation, the supernatant was collected (negative selection), and hPSA-MPs were added to the supernatant in such a way that the ratio of protein/DNA was 1:10. After interaction and magnetic separation, the supernatant was discarded (positive selection) and the particles were washed with BSL buffer (BS + 0.01% tween-20). The bound DNA was eluted by incubation with 30 μL of water at 95 °C for 15 min and magnetic separation. All the incubations were performed at 25 °C and 1300 rpm. 2 μL of eluted DNA were PCR amplified with 1 μM biotinylated reverse primer, 1 μM 6-FAM- forward primer (Table S1), 3 mM $MgCl_2$, 0.2 mM dNTPs and 1 U hot-start immolase™ DNA polymerase. The protocol was as follows: 95 °C for 10 min to activate the enzyme, then 15 cycles of 94 °C for 45 s, 57 °C for 45 s and 72 °C for 45 s; and a final step at 72 °C for 10 min. The DNA amplified was run in a 2% agarose gel to check that the amplified DNA had the expected size. The concentration of amplified dsDNA was quantified by fluorescence. When less than 250 pmol of DNA was obtained, a new aliquot of DNA was amplified by PCR.

The strand separation from 250 pmol of the amplified DNA was performed using Dynabeads MyOne Streptavidin C1 magnetic particles (Invitrogen). They were washed 3 times with BLstrep buffer (10 mM Tris-HCl 2 M NaCl + 0.01% tween-20) and then resuspended in the same buffer without tween-20 in a volume equal to the volume of DNA to separate. After 15 min of interaction, the beads were washed 3 times with BLstrep and then incubated with 50 μL of 100 mM NaOH for 10 min to release the unbound strand. After magnetic separation, the supernatant was collected, neutralized with 1 M HCl and diluted with BS to start a new round.

To direct the selection toward the glycosylation site of the protein two counter-selections were performed in round 3 and 6. They consisted on the incubation of the DNA with rPSA-MPs. After the interaction and magnetic separation, the supernatant was collected and incubated with hPSA-MPs as indicated above.

The incubation time was decreased and the washing steps were increased in each round as indicated in Table S2. Concentrations of competitor and BSA were modified accordingly to the DNA concentration. After six rounds of selection, the remaining DNA was identified by next-generation sequencing. Enrichment assays through the selection, sequencing analysis and protocols for aptamer binding characterization are included in the Supporting information.

2.3. Sandwich assay

To fabricate the sensors, the capture biotinylated aptamer (biotin-anti-PSA) was immobilized through the biotin-streptavidin interaction on screen-printed gold electrodes (SPAuE) (DRP-220BT, Metrohm-Dropsens, Spain) modified with a mixed self-assembled monolayer (SAM), obtained after overnight incubation at 4 °C in a 1:3 mixture of 11-mercaptoundecanoic acid (1 mM in ethanol) and mercaptohexanol (1 mM in ethanol). First, the carboxylic groups of the SAM were activated with a mixture of 100 mM EDC and 25 mM NHS in water for 30 min, and then we added streptavidin (50 μg/mL) in NaAc buffer for 30 min. The remaining activated groups were blocked with 1 M ethanolamine in PBS 1 × for 15 min, and finally the surface was incubated with 1 μM biotin-anti-PSA in TBS (10 mM Tris-HCl, 150 mM NaCl, 5 mM KCl, 5 mM $MgCl_2$ pH 7.4) for 30 min.

For PSA analysis, serial dilutions of standard PSA in TBS or serum were incubated on the working electrode for 30 min and then the detection aptamer, 1 μM 6FAM-PSA1 in TBS was added for 30 min. The labeling and detection steps were performed as described for the binding assays (Supporting Information). After each step, the electrode was washed with the buffer used in the following step and dried with nitrogen. Volumes of 10 μL were used, and incubations were performed at room temperature. When handling numerous modified electrodes, the initial step was wisely delayed to keep a strict control on timing.

3. Results and discussion

3.1. Selection of aptamers

Our approach to isolate novel DNA aptamers targeting hPSA with intrinsic preference for the glycosylation site relies on the introduction of counter-selection steps using rPSA that does not carry the glycan moiety. The counter-selection is performed once the DNA library begins to enrich in sequences recognizing the glycosylated protein previous subtraction of sequences with affinity for the BSA-blocked MPs without target, that is, BSA-MPs (negative or subtractive selection) (Fig. 1). Introducing negative steps in all rounds is not very common but has already been reported (Kimoto et al., 2013). We advise against this practice when the target is not highly “aptagenic” to avoid removing most initial sequences (Svigelj et al., 2018) but in this case we reasoned it would be wise to increase the stringency because there are two proteins on the hPSA-MPs during the positive selection. Thus, after 2 rounds of selection against the whole protein we started the next selection cycle by incubating the amplified sequences with rPSA-MPs. In this way, we selectively removed those sequences that recognize the protein at regions different from the glycosylation site, subjecting the remaining ones to a new interaction with hPSA (third round). Next, we performed two classical selection cycles and before the sixth round we repeated the counter-selection.

Pool enrichment was monitored by using fluorescein as a tracer, incorporated during PCR steps, for measuring the percentage of oligonucleotides retained by the immobilized hPSA after each round of selection (Fig. 2A). We observed a progressive enrichment of the DNA library in sequences with affinity toward hPSA, and after 6 rounds of selection, 60% of the oligonucleotides were bound to the immobilized glycoprotein, indicating a high percentage of specific binders for PSA in this pool. In contrast, a dramatic decrease in affinity for the rPSA is apparent in rounds 3 and 6 showing the effectiveness of counter-selection steps performed in those cycles.

We next evaluated the average binding affinity of the oligonucleotide pools selected after each round. hPSA was chemically bound to gold SPR disks and incubated with serial dilutions of PCR amplified pools. Fig. 2B shows virtually no binding with the initial library and an increased binding affinity to hPSA as selection progresses. In the 5th round a small signal appears at 100 nM while a much higher signal is observed at the lowest concentration tested (10 nM) in the 6th round. To study whether binding actually involves the glycosylation site, we repeated the experiment with the pool 6 and rPSA on the SPR sensor. The displacement of the binding curve toward higher aptamer concentrations indicates that oligonucleotides in this pool recognize the unglycosylated form but with significantly lower affinity. These results suggest that a high percentage of the sequences in the last round indeed bind to PSA through preferential recognition of the glycan in good agreement with fluorescent assays.

Next-generation sequencing allowed us to identify sequences from several rounds and analyze them. The in vitro selection changes the observed nucleotides abundance, with a slight bias toward dG and dT enrichment (Fig. S1). The starting DNA library did not contain an even distribution of the nucleotides as expected, with a composition of 27.41% dA, 27.65% dT, 23.76% dC and 21.19% dG for all the sequences analyzed (326,411 reads). On the contrary, in the sixth round we obtained 304,722 reads with an enrichment in dG (27.08%) and dT (28.26%). The distribution of the nucleotides at each position of the random region in the last round pool indicates an increase in dT at 3’ end while G dominates the 5’ end (Fig. S2). The sequence complexity, estimated as the relative amount of unique sequences to total reads

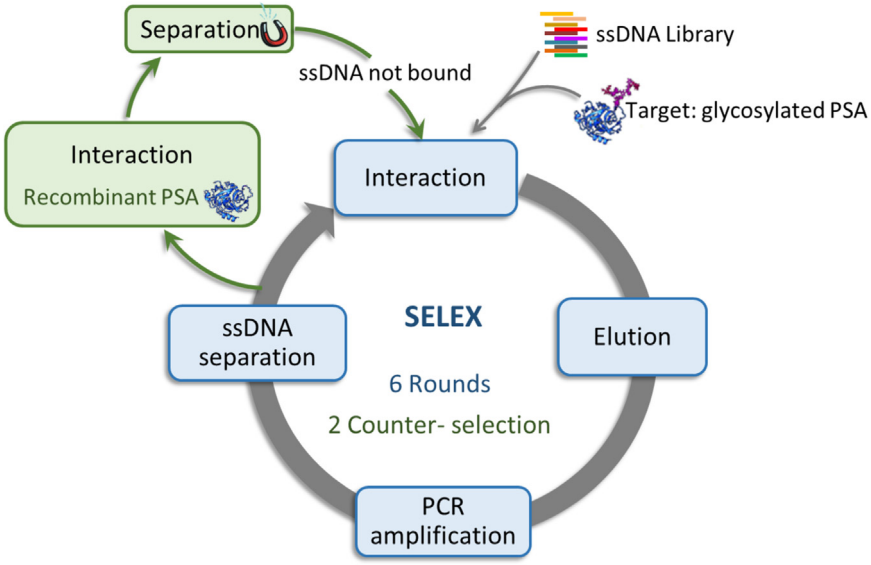

Fig. 1. Scheme of the SELEX procedure followed in this work to direct the selection toward the glycan chain.

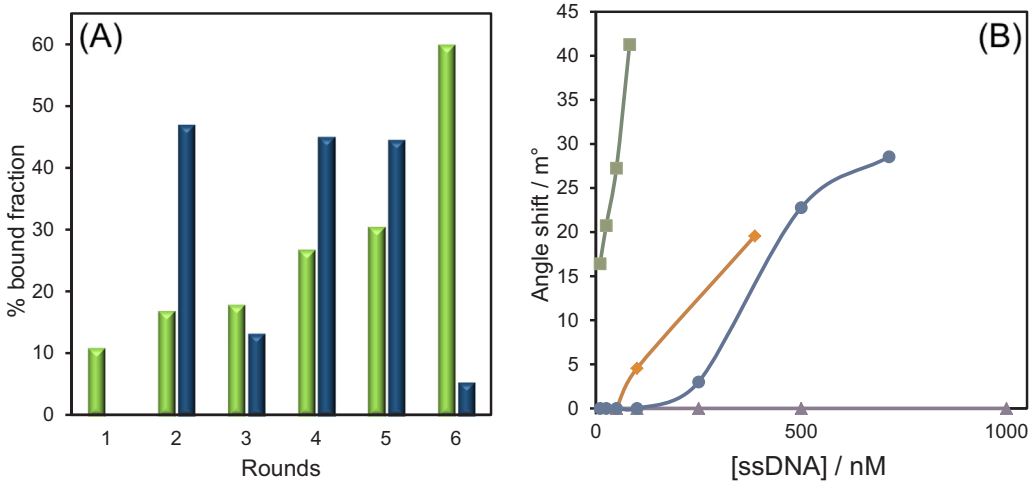

Fig. 2. Enrichment assays. A) Evolution of the percentage of DNA that binds to hPSA (light green) and rPSA (dark blue) through the SELEX rounds obtained by fluorescence measurements. B) SPR measurements obtained with increasing concentrations of DNA from round cero (purple triangles), five (orange diamonds) and six (green squares) for the hPSA and comparison with the results from round six for the rPSA (blue circles). (For interpretation of the references to color in this figure legend, the reader is referred to the web version of this article).

within each round (% complexity = unique/total), decreased from 0.19% in round 2 pool to 0.09% in the last pool. Diversity changes were monitored by melting curve analysis after a short reannealing of 30 s at 50 °C (Vanbrabant et al., 2014). A shift in the re-melting temperature from 81.7 °C in the starting library to 82.7 °C in the round 6 was found, which is in agreement with a decrease in the diversity of the oligonucleotide pool. (Fig. S3).

In order to study the evolution of sequences during the rounds, the identified oligonucleotides from round 0, 2, 4 and 6 were compiled into a non-redundant aptamer database and the sequences that were kept throughout the SELEX were classified into families, obtaining a family tree (Fig. S4). Next, each family was further analyzed to identify repetitive motifs. Since a ten-fold increase in affinity has been associated to 5 conserved positions (Carothers et al., 2006) we selected the four out of seven families with motifs containing at least 5 unambiguous nucleotides (low variable or high consensus sequences). (Table S3). These motifs are highly recurrent in the pool according to the total number of repetitions found. The structure of potential aptamers from each family was predicted using Mfold (Zucker, 2003), selecting as candidates those with the lowest free energy (more stable secondary structures) (Fig. S5). Note that though nature tends to provide the simplest solution, intricate nucleic acid structures are more informational complex and are positively correlated with lower K_D (higher affinity) (Carothers et al., 2006). Additionally, the most repeated sequence (highest copy number) was also selected for further characterization (see the five sequences in Table S4). The candidate aptamers were synthesized including 5 thymines as a spacer in the 5'-end of the selected sequences (40 nt central sequences).

3.2. Characterization of the candidate aptamers

Individual ability to bind both hPSA and rPSA was first tested using an electrochemical binding assay with chronoamperometric detection. These proteins were immobilized onto screen-printed gold electrodes (SPAuE) and incubated with a 500 nM solution of each aptamer labeled with fluorescein. After the affinity interaction, fluorescein was tagged with the enzyme conjugate Fab-anti fluorescein-POD, and the amount of immobilized enzyme was measured by chronoamperometry at 0.2 V. All aptamers recognized hPSA but with different affinity (Fig. 3A). PSA-5, the most abundant one, showed the highest analytical signal toward hPSA but it also recognized rPSA (60% of the hPSA signal). PSA-1 is the aptamer showing the lowest signal towards rPSA, and the highest discrimination ability between glycosylated and unglycosylated forms of the protein, which points to the recognition through the glycosylation site. PSA-2 also preferentially binds to hPSA but the signal is 33% lower than PSA-1 aptamer. Conversely, PSA-3 binds the recombinant protein much stronger than the human one. PSA-4 shows similar recognition ability for both proteins within the experimental error.

The affinity of PSA-1 toward hPSA was evaluated in more detailed by building the binding curve with increasing concentrations of aptamer. The curve fitted well to the Langmuir model, which assumes a 1:1 stoichiometry, that is, a single binding site per protein, providing a dissociation constant of 357 ± 42 nM. (Fig. 3B). This value is lower than the average obtained with pool 6 under identical conditions (K_D = 480 ± 44 nM) suggesting that PSA-1 is among the strongest binders in the pool. Of note, the affinity constant is at least one order of magnitude better than that described for lectins; for example the affinity for a core-fucose specific lectin ranged from 3.2 to 22 μM obtained by frontal affinity chromatography, a technique specifically designed for analysis of weak interactions (Kobayashi et al., 2012). Recently, a strong binding, K_D in the low nM range, was reported for some lectins interacting with PSA glycans by SPR (Damborský et al., 2016) but these values cannot be directly compared with our results. Unlike aptamers, all these lectins are oligomers so they can bind to several proteins on a surface (multivalency). K_D values dependent on protein density are expected and demonstrated on microarray experiments with lowest K_D at high densities. SPR K_D values are reported for protein densities as high as 6.13 ng/mm^2 while our results come from 1.6 ng/mm^2 as the upper limit.

For the sake of comparison with the aptamer already described in the literature for hPSA (Savory et al., 2010), denoted here as anti-PSA aptamer, a K_D value of 229 ± 25 nM was estimated with our electrochemical binding assay. Previously, a value of 37 nM was obtained by quartz-crystal microbalance (Formisano et al., 2015).

It is now accepted that robust aptamer characterization requires the use of several techniques because the variable response depending on the sensitivity of the technique and the effect of the immobilization strategy when needed (McKeague et al., 2015; Miranda-Castro et al., 2018). It has been also openly recognized that aptamers work dissimilarly in different analytical assays (Li et al., 2009). Consequently, we also investigated the affinity of the different aptamers by SPR. Au-SPR chips were modified with hPSA and incubated with increasing concentrations of aptamer. Dissociation constants for PSA-1, and anti-PSA were 177 ± 65 nM and 177 ± 5 nM, respectively. The discrepancy with the electrochemical estimation could be ascribed to the deleterious effect of labeling. In principle, the fluorescein tag is not expected to impact on affinity because the selection was performed with tagged-aptamers to minimize it. However, the labeling with a bulky enzyme conjugate could cause that only a fraction of aptamers bound to PSA would be accessible (the parking problem) limiting the sensitivity. It has been argued that the flexibility of sugar structure limits the affinity of the receptors as in the case of lectins. We have shown that aptamer

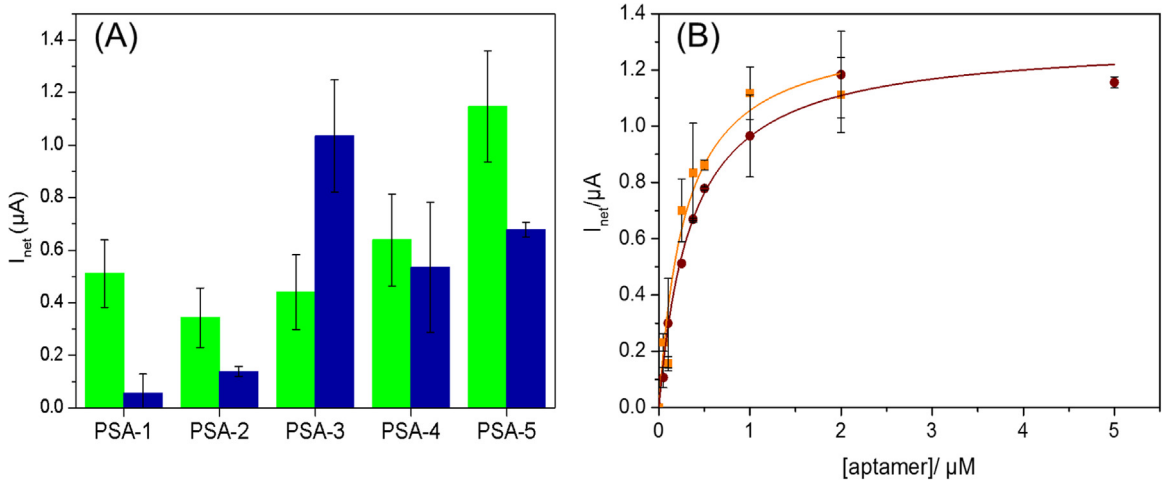

Fig. 3. A) Current intensities obtained by chroanomperometry at + 0.2 V on SPAuE modified with hPSA (light green) and rPSA (dark blue) using 500 nM of 6-FAM-aptamers. B) Binding curves obtained by chronoamperometry on hPSA-modified SPAuE for PSA-1 aptamer (circles) and anti-PSA (squares). (For interpretation of the references to color in this figure legend, the reader is referred to the web version of this article).

directed selection could overcome this limitation. Glycan-binding aptamers with as low affinities as protein-binding aptamers are feasible to obtain.

As a second test for the ability of PSA-1 to recognize the protein by the glycan structure, a distinctive characteristic that may be not achieved by anti-PSA that was selected by a non-directed SELEX process, we repeated the binding experiment but challenging both aptamers to rPSA. The anti-PSA showed preferential binding to rPSA (K_D = 70 ± 5 nM) suggesting that it recognizes the protein but in a region that is perturbed by the glycan or folded into a different conformation after post-translation modification. On the contrary, PSA-1 gave no significant signal in SPR studies, even at the highest concentration tested (1 μM), which is consistent with the recognition of the carbohydrate moiety in the protein we have already observed in the electrochemical experiment.

In contrast to PSA-1, the experimental results obtained by challenging immobilized hPSA, either on SPR disks or on AuSPE, with increasing concentrations of the aptamer PSA-5 are well fitted to the Hill equation, with K_D values of 144 ± 65 nM and 209 ± 16 nM obtained by electrochemical and SPR measurements, respectively. This presumably reflects the cooperative binding of PSA-5, which is in agreement with the increased responses observed with this aptamer. Nevertheless, PSA-5 exhibited reduced ability to discriminate between hPSA and rPSA when compared to PSA-1.

The selectivity of PSA-1 aptamer was challenged on SPAuE modified with lipocalin-2 (NGAL), a single-glycosylated small protein. A concentration of 500 nM of fluorescein-labeled aptamer showed a current identical within the experimental error to the one for PSA. The signals obtained were 743 ± 63 nA for NGAL and 779 ± 133 nA for hPSA, meaning that this aptamer binds to the glycan moiety so it might be a general reagent for human carbohydrate chains on proteins.

3.3. PSA detection in a sandwich assay format

It is quite intriguing that sandwich assays with two aptamers are rare and limited to a few targets, though the selection process always yields several high-affinity winning sequences. This is probably because the requirements are more restrictive for aptamers than antibodies. Not only the protein must have two different aptatopes (or two identical but distant ones) but also the DNA sequence complementarity must be as low as possible to avoid undesired hybridization and the related high background signals. Preliminary electrochemical experiments using the previously described anti-PSA as both capture and detection aptamers revealed a S/B ratio close to 1 suggesting there is no two binding sites, in good agreement with recently reported attempts to develop an aptasandwich assay (Li et al., 2018). Additionally both currents are higher than the signal obtained when no detection aptamer was added indicating that hybridization takes place to some extent. Using Mfold web server we estimated the hybridization free energy and the melting temperature (T_m) of all possible homo and hetero-combinations with PSA-1, PSA-5 and antiPSA (Table S6), which confirms this and other hybridizations. The less stable duplex is achieved with PSA-1 and antiPSA due to the low absolute value of free energy and T_m. For this reason, a sandwich assay with the anti-PSA and PSA-1 aptamers was designed to the quantification of PSA. Anti-PSA aptamer was immobilized onto SPAuE through the streptavidin-biotin interaction to act as a capture aptamer (Fig. 4A). The SAM on which the sensing surface is built precludes most unspecific interactions with the electrode material, a common problem in these devices. After the interaction with increasing concentrations of hPSA, 6-FAM-PSA-1 aptamer was used as a detection aptamer and the chronoamperometric current was recorded as indicated in previous experiments. It is of paramount importance that analytical assays using aptamers are performed under conditions as similar as possible to the selection. In this case, the optimum buffer for PSA binding to anti-PSA is different from the selection buffer used in our SELEX, which could be inconvenient if one of the aptamers is susceptible to buffer variability. Preliminary experiments showed that our aptamers maintain their affinity for hPSA in TBS. As an example, using 500 nM of PSA-1 the net current obtained in PBS and in TBS buffer were 779 ± 133 nA and 1570 ± 415, respectively. So we decided to use the anti-PSA buffer to maximize the performance of the capture aptamer that will have to entrap the protein in an ocean of other compounds.

As expected, an increasing response was observed in the range from 0.66 ng/mL to 62.5 ng/mL in TBS buffer (Fig. 4B upper panel). The signal was normalized by expressing the percentage of the maximum net current to account for inter-day variations. Mostly overlapped calibration curves are obtained in successive days indicating the robustness of the normalization so the Fig. 4B shows the averaged calibration curve of all of them. The calibration range was narrower in serum diluted 1:1 with TBS buffer (0.66 ng/mL to 25 ng/mL), but in both conditions it covers the grey zone, 4–10 ng/mL of PSA in serum. The calibration curve fitted well to the Langmuir equation $y = (y_o \cdot x)/ (y_{max} + x)$, with a y_o value of 1.06 ± 0.09% and y_{max} of 100 ± 2% with a correlation of 0.998. The limit of detection, 0.66 ng/mL, was estimated as the concentration corresponding to a signal that is three times the standard deviation of the blank. This value compares well and even surpassed the only report attempting the PSA glycoprofiling using an aptamer as a capture reagent (anti-PSA as herein) showing that our

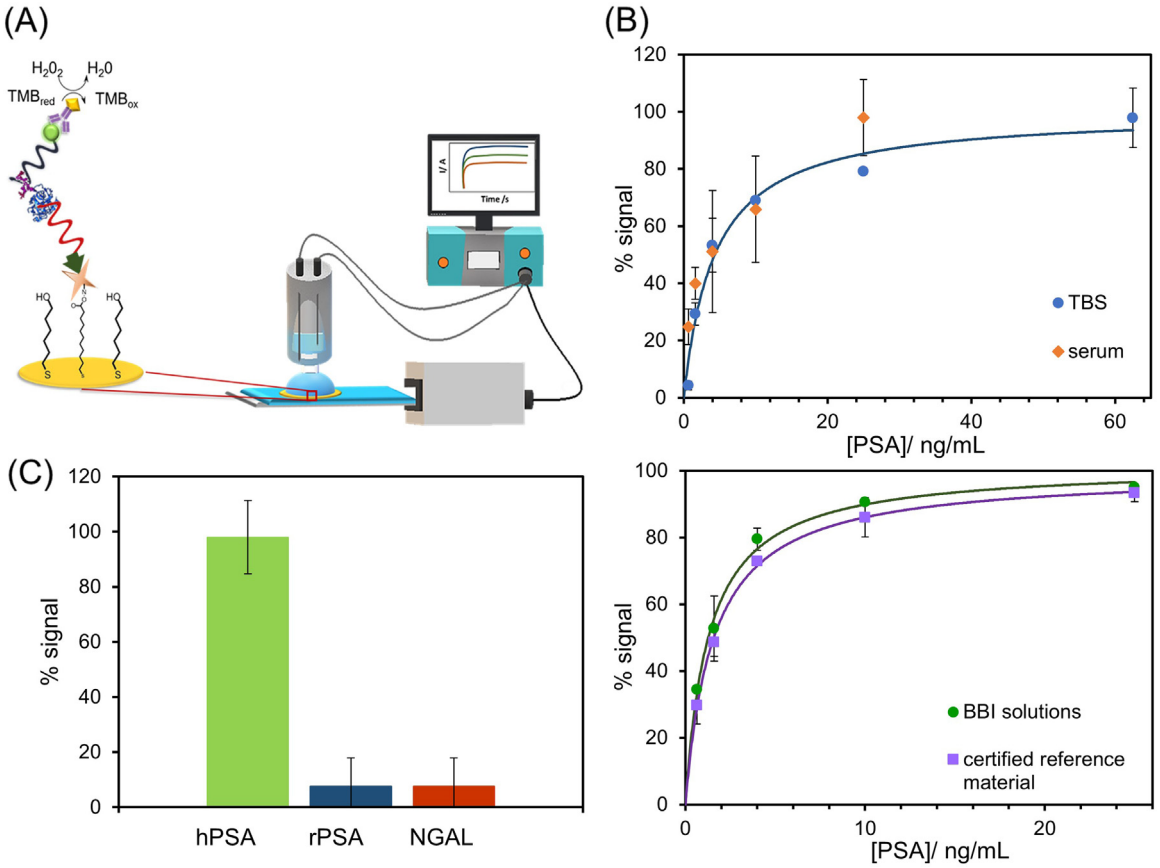

Fig. 4. A) Scheme of the sandwich assay, B) calibration plots of PSA in TBS, diluted serum 1:1 with TBS (upper panel) and two different PSA standards (bottom panel), and C) sensor response to 25 ng/mL of hPSA, rPSA and the glycoprotein NGAL.

novel aptamer is superior than lectins to detect the glycan portion (Jolly et al., 2016). Very recently a novel anti-PSA aptamer was selected and used in a sandwich configuration because there were two separated binding sites on the protein. Unfortunately, the assay was not sensitive enough to detect PSA at clinically relevant levels (Li et al., 2018). Nonetheless, our efforts were not focused to sensitivity but to the real applicability in patients' samples as demonstrated below. There are a myriad of novel PSA sensors reported in the last years. As an example in a quick search 79 matches were retrieved from Scopus database with input words being PSA and aptamer since 2010; 38 if "electrochemical" is added. Similar results were obtained from SciFinder with 104 answers matching PSA aptamer, 86 journal articles and 18 patents. All this effort has been summarized recently (Damborska et al., 2017) showing that extremely difficult to defeat limits of detection has been achieved, 0.96–20 ag/mL (32–660 zM) (Hao et al., 2017; Tang et al., 2015; Zhu et al., 2016) though the need for such sensitivity is unclear.

Contrarily, discordant results obtained in clinical laboratories when different PSA standards or ELISA methods are used are frequently set aside in most of these publications but they are well described in the literature (McJimpsey, 2016; Stephan et al., 2009). In fact, follow-up measurements to monitor recurrence could be challenging if they are obtained from different laboratories. To check the robustness of our sandwich assay we constructed a calibration curve with a certified reference material. The standard was reconstituted in water and then diluted in 1:1 TBS-serum and analyzed with the sandwich assay above described. The calibration curve, also expressed as the percentage of the maximum signal obtained, was not significantly different from the calibration with the non-certified commercial PSA source (Fig. 4B bottom panel), which renders this sensing architecture a promising tool for clinical applications.

3.4. Selectivity of the sandwich assay in serum

Initial selectivity studies were limited to rPSA and NGAL that is also a glycoprotein at 25 ng/mL in serum. In both cases, the net current obtained is significantly lower than the one obtained for the same concentration of PSA (Fig. 4C). Note that the detection aptamer recognizes the glycan on NGAL but the sandwich format secures the selectivity of the assay against other glycoproteins than PSA.

A broad-spectrum selectivity study was designed by analyzing two control standards containing an array of 92 analytes including total and free PSA (Table S6) at two levels. The lyophilized control was reconstituted with water, then diluted 1:1 with TBS buffer and analyzed with the sensor as previous described.

The results summed up in Table 1 show that the electrochemical sensor provides a concentration of PSA that agreed with the value for the total PSA concentration of the control indicating that not only fPSA but also combined PSA can be captured by anti-PSA and PSA-1 aptamers. The sensor does not present significant interferences even in the presence of a great variety of molecules at physiological level.

Table 1
Selectivity of the sandwich assay.

Control	Concentration found	Concentration BIO-RAD control	
		fPSA	tPSA
Level 2	1.9 ± 0.4 ng/mL	1.06 ± 0.05 ng/mL	1.88 ± 0.1 ng/mL
Level 3	14 ± 3 ng/mL	9.7 ± 0.5 ng/mL	15.5 ± 0.9 ng/mL

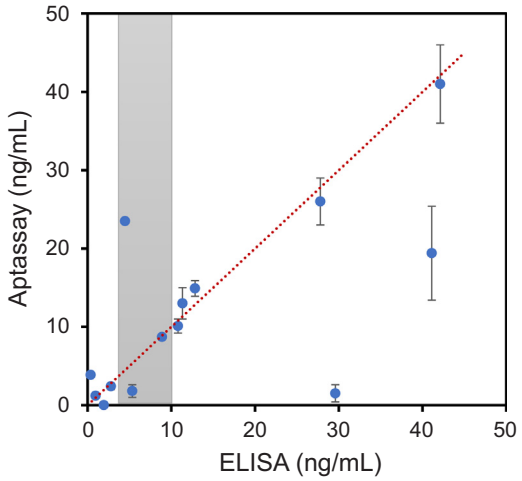

Fig. 5. Concordance of the ELISA and aptasensor methods in the determination of total PSA in serum samples. 14 out of 15 analyzed samples are plotted. The 15th sample gave similar results by ELISA (93.9 ng/mL) and aptasensor (91 ± 8 ng/mL). Grey PSA-concentration zone is emphasized in grey.

3.5. Analysis of PSA in clinical samples

To investigate the diagnostic value of the aptamer-based assay, the sensor was challenged in serum samples from 15 patients with different levels of total PSA. The samples were diluted with TBS buffer and analyzed using the sandwich assay protocol described without any other pretreatment. The sera were also assayed in the central labs of Hospital de Cabueñes using the automated ADVIA Centaur® (Siemens) ELISA assay for the quantification of total PSA. The values obtained are summarized in Fig. 5.

The sensor results are concordant with those obtained by ELISA in 60% of samples, presumably due to the differences in the glycan profiles of the analyzed samples. Out of six discordant samples, four gave a low aptasensor value compared with the ELISA assay. Total PSA is elevated in serum in not only men with prostate cancer but also in cases of benign prostatic hyperplasia (BPH) or prostatitis.

Two of the discordant results having a higher PSA value by ELISA were finally diagnosed of BPH (ELISA value 29.6 ng/mL) and diabetes mellitus type II (ELISA value 5.3 ng/mL). Our sensor correctly classified them below the grey zone, showing superior selectivity. The third discordant value corresponded to a prostate neoplasia and our sensor also correctly identified it above 10 ng/mL cutoff but not as high as ELISA (41.1 vs. 19.4 ng/mL). The fourth one had a value close to the limit of detection by ELISA, which was undetectable by the aptasensor.

The remaining two discordant samples presented elevated values by aptasensor. While one of them showed PSA values below the 4 ng/mL threshold by both methods, which is not problematic, the second one was slightly over this threshold by ELISA but much higher by our method. The final diagnosis of this patient was prostatitis. Very high PSA values have been reported for this disease before implementing an antibiotic treatment but the values are recovered after treatment (Hara et al., 2004), so this high value is not unexpected. Taken together, the discrepant results are reasonable explained assuming different glycosylation patterns for several diseases. Although the number of samples analyzed is small, these preliminary results point to the usefulness of the aptamer-based assay to improve PSA test specificity. Ongoing research in our labs is devoted to elucidate this open and exciting question beyond the scope of this work.

4. Conclusions

We demonstrate the ability to direct the aptamer selection toward the glycan structure of a glycoprotein via counter-selection steps against a recombinant unglycosylated form of the target. Using this approach and aided with deep sequencing, after only six rounds of selection with two counter-selection steps we identified an aptamer recognizing the glycan moiety in PSA, discriminating hPSA from rPSA. This approach should offer a powerful general tool for the selection of aptamers for glycoproteins with the glycan structure as aptatope.

The selected aptamer was employed to design an aptamer-based sensor with a sandwich format to detect hPSA. The sensor supports the measurement in serum samples with a minimal dilution and a limit of detection of 0.66 ng/mL, which allows the evaluation of PSA levels with clinical significance in the diagnosis of prostate cancer.

The results obtained with the sensor for serum of patients with benign prostate hyperplasia are lower than those obtained with the standard ELISA, which suggests that the sensor detects a fraction of PSA with a distinct glycan structure. The proposed aptasensor could provide an alternative approach for the detection of PSA, with potential to improve clinical outcomes of PSA tests and to reduce the number of unnecessary biopsies for the diagnosis of prostate cancer.

CRediT authorship contribution statement

Ana Díaz-Fernández: Conceptualization. **Rebeca Miranda-Castro:** Conceptualization. **Noemí de-los-Santos-Álvarez:** Conceptualization. **Eloy Fernández Rodríguez:** Validation. **María Jesús Lobo-Castañón:** Conceptualization, Supervision.

Acknowledgments

This work was funded by the Spanish Ministerio de Economía y Competitividad through Project No. CTQ2015-63567-R and co-financed by FEDER funds. A.D.F. was supported by Asociación Española Contra el Cáncer (AECC) with a Ph.D. fellowship.

Declaration of competing interests

None.

Appendix A. Supporting information

Supplementary data associated with this article can be found in the online version at doi:10.1016/j.bios.2018.12.040.

References

Carothers, J.M., Oestreich, S.C., Szostak, J.W., 2006. J. Am. Chem. Soc. 128, 7929–7937.
Cha, T., Cho, S., Kim, Y.T., Lee, J.H., 2014. Biosens. Bioelectron. 62, 31–37.
Damborska, D., Bertok, T., Dosekova, E., Holazova, A., Lorencova, L., Kasak, P., Tkac, J., 2017. Microchim. Acta 184, 3049–3067.
Damborský, P., Zámorová, M., Katrlík, J., 2016. Proteomics 16, 3096–3104.
Díaz-Fernández, A., Miranda-Castro, R., de-los-Santos-Álvarez, N., Lobo-Castañón, M.J., 2018. Anal. Bioanal. Chem. 410, 2059–2065.
Eissa, S., Zourob, M., 2017. Sci. Rep. 7, 1016.
Formisano, N., Jolly, P., Bhalla, N., Cromhout, M., Flanagan, S.P., Fogel, R., Limson, J.L., Estrela, P., 2015. Sens. Actuators B 220, 369–375.
Gilgunn, S., Conroy, P.J., Saldova, R., Rudd, P.M., O'Kennedy, R.J., 2013. Nat. Rev. Urol. 10, 99–107.
Hanahan, D., Weinberg, R.A., 2011. Cell 144, 646–674.
Hao, T., Wu, X., Xu, L., Liu, L., Ma, W., Kuang, H., Xu, C., 2017. Small 3, 1603944.
Hara, N., Koike, H., Ogino, S., Okuizumi, M., Kawaguchi, M., 2004. Prostata 60, 282–288.
Hayes, J.H., Barry, M.J., 2014. JAMA 311, 1143–1149.
Heydari-Brafrooei, E., Shamszadeh, N.S., 2017. Biosens. Bioelectron. 91, 284–292.
Hsieh, P.-C., Lin, H.-T., Chen, W.-Y., sai, J.J.P., Hu, W.-P., 2017. BioMed. Res. Int. 5041683.
Jeong, S., Han, S.R., Lee, Y.J., Lee, S.-W., 2010. Biotechnol. Lett. 32, 379–385.
Jolly, P., Damborsky, P., Madaboosi, N., Soares, R.R.G., Chu, V., Conde, J.P., Katrlik, J., Estrela, P., 2016. Biosens. Bioelectron. 79, 313–319.
Kimoto, M., Yamashige, R., Matsunaga, K., Yokoyama, S., Hirao, I., 2013. Nat. Biotechnol. 31, 453–457.
Kobayashi, Y., Tateno, H., Dohra, H., Moriwaki, K., Miyoshi, E., Hirabayashi, J., Kawagishi, H., 2012. J. Biol. Chem. 287, 33973–33982.
Li, M., Guo, X., Li, H., Zuo, X., Hao, R., Song, H., Aldalbahi, A., Ge, Z., Li, J., Li, Q., Song, S., Li, S., Shao, N., Fan, C., Wang, L., 2018. ACS Appl. Mater. Interfaces 10, 341–349.

Li, M., Lin, N., Huang, Z., Du, L., Altier, C., Fang, H., Wang, B., 2008. J. Am. Chem. Soc. 130, 12636–12638.
Li, Na, Ebright, J.N., Stovall, G.W., Chen, X., Nguyen, H.H., Singh, A., Syrett, A., Ellington, A.D., 2009. J. Prot. Res. 8, 2438–2448.
Li, Y., Tao, S.-C., Bova, G.S., Liu, A.Y., Chan, D.W., Zhu, H., Zhang, H., 2011. Anal. Chem. 83, 8509–8516.
Lilja, H., Ulmert, D., Vickers, A.J., 2008. Nat. Rev. Cancer 8, 267–278.
McJimpsey, E.L., 2016. Sci. Rep. 6, 1–8.
McKeague, M., De Girolamo, A., Valenzano, S., Pascale, M., Ruscito, A., Velu, R., Frost, N.R., Hill, K., Smith, M., McConnell, E.M., DeRosa, M.C., 2015. Anal. Chem. 87, 8608–8612.
Meany, D.L., Zhang, Z., Sokoll, L.J., Zhang, H., Chan, D.W., 2009. J. Proteome Res. 8, 613–619.
Miranda-Castro, R., de-los-Santos-Álvarez, N., Lobo-Castañón, M.J., 2016. Aptamers as synthetic receptors for food quality and safety control. In: Scognamiglio, V., Arduini, F., Palleschi, G. (Eds.), Biosensors for Sustainable Food- New Opportunities and Technical Challenges. Comprehensive Analytical Chemistry 74. Elsevier, Amsterdam, pp. 155–191.
Miranda-Castro, R., de-los-Santos-Álvarez, N., Lobo-Castañón, M.J., 2018. Characterization of aptamer-ligand complexes. In: Dong, Y. (Ed.), Aptamers for Analytical Applications: Affinity Acquisition and Method Design. Wiley, Weinheim, pp. 127–172. https://doi.org/10.1002/9783527806799.
Munkley, J., Elliot, D.J., 2016. Oncotarget 7, 35478–35489.
Park, J.-W., Lee, S.J., Ren, S., Lee, S., Kim, S., Laurell, T., 2016. Sci. Rep. 6, 27121.
Pihíková, D., Belicky, S., Kasák, P., Bertok, T., Tkac, J., 2016. Analyst 141, 1044–1051.
Rose, C.M., Hayes, M.J., Stettler, G.R., Hickey, S.F., Axelrod, T.M., Giustin, N.P., Suljak, S.W., 2010. Analyst 135, 2945–2951.
Saldova, R., Fan, Y., Fitzpatrick, J.M., Watson, R.W.G., Rudd, P.M., 2011. Glycobiology 21, 195–205.
Savory, N., Abe, K., Sode, K., Ikebukuro, K., 2010. Biosens. Bioelectron. 26, 1386–1391.
Siegel, R.L., Miller, K.D., Jemal, A., 2018. CA Cancer J. Clin. 68, 7–30.
Stephan, C., Bangma, C., Vignati, G., Bartsch, G., Lein, M., Jung, K., Philippe, M., Semjonow, A., Catalon, W.J., 2009. Int. J. Biol. Markers 24, 65–69.
Souada, M., Piro, B., Reisberg, S., Anquetin, G., Noël, V., Pham, M.C., 2015. Biosens. Bioelectron. 68, 49–54.
Svigelj, R., Dossi, N., Toniolo, R., Miranda-Castro, R., de-los-Santos-Álvarez, N., Lobo-Castañón, M.J., 2018. Angew. Chem. Int. Ed. 57, 12850–12854.
Svobodova, M., Bunka, D.H.J., Nadal, P., Stockley, P.G., O'Sullivan, C.K., 2013. Anal. Bioanal. Chem. 405, 9149–9157.
Tabarés, G., Radcliffe, C.M., Barrabés, S., Ramírez, M., Aleixandre, R.N., Hoesel, W., Dwek, R.A., Rudd, P.M., Peracaula, R., de Llorens, R., 2006. Glycobiology 16, 132–145.
Tamboli, V.K., Bhalla, N., Jolly, P., Bowen, C.R., Taylor, J.T., Bowen, J.L., Allender, C.J., Estrela, P., 2016. Anal. Chem. 88, 11486–11490.
Tzouvadaki, I., Jolly, P., Lu, X., Ingebrandt, S., de Micheli, G., Estrela, P., Carrara, S., 2016. Nano Lett. 16, 4472–4476.
Vanbrabant, J., Leirs, K., Vanschoenbeek, K., Lammertyn, J., Michiels, L., 2014. Analyst 139, 589–595.
Yang, J., Hu, Y., Dong, N., Zhu, G., Zhu, T., Jiang, N., 2017. Biosens. Bioelectron. 94, 286–291.
Zhao, J., Ma, Z., 2018. Biosens. Bioelectron. 102, 316–320.
Tang, L., Li, S., Xu, L., Ma, W., Kuang, H., Wang, L., Xu, C., 2015. ACS Appl. Mater. Interfaces 7, 12708–12712.
Zhu, Y., Wang, H., Wang, L., Zhu, J., Jiang, W., 2016. ACS Appl. Mater. Interfaces 8, 2573–2581.
Zucker, M., 2003. Nucleic Acids Res. 31, 3406–3415.